Photoactivated Linkage Isomerism in Single Crystals of Nickel, Palladium and Platinum Di-nitro Complexes – A Photocrystallographic Investigation

Mark R. Warren,[a] Simon K. Brayshaw,[a] Lauren E. Hatcher,[a] Andrew L. Johnson,[a,*] Stefanie Schiffers,[a] Anna J. Warren,[a] Simon, J. Teat,[b] John E. Warren,[c] Christopher H. Woodall[a] and Paul R. Raithby[a,*]

Received (in XXX, XXX) Xth XXXXXXXXX 200X, Accepted Xth XXXXXXXXX 200X
First published on the web Xth XXXXXXXXX 200X
DOI: 10.1039/b000000x

Low temperature, single crystal photocrystallographic studies have been carried out on four square planar Group 10 complexes $[Ni(PEt_3)_2(NO_2)_2]$ **1**, $[Pd(PPh_3)_2(NO_2)_2]$ **2**, $[Pd(AsPh_3)_2(NO_2)_2]$ **3** and $[Pt(PPh_3)_2(NO_2)_2]$ **4**, in which the two nitro groups adopt the *trans* configuration. Irradiation with UV light, at 100 K, of single crystals of complexes **1**-**3** photoisomerise from the η^1-NO_2 nitro form to the η^1-ONO nitrito form occurred. Complex **1** underwent 25% conversion to the nitrito form before crystal decomposition occurred. **2** and **3** underwent 46% and 39% conversion, respectively, to the nitrito form when a photostationary state was reached. While under the same experimental conditions **4** showed no isomerisation. The photocrystallographic results can be correlated with the results of DFT calculations and with the observed trends in the solution UV/visible absorption spectroscopy obtained for these complexes. The results suggest that while steric factors in the isomerization processes are important there may also be a kinetic effect relating to the lability of the metal involved.

Introduction

With the dramatic advances in X-ray crystallographic techniques the field of Photocrystallography[1] has grown rapidly over the last two decades. The power of the technique in allowing the full, three-dimensional structure determination of photoactivated species within a crystalline lattice has encouraged its application in a variety of solid-state photochemical processes. Examples of photocrystallographic studies in inorganic and molecular chemistry include light-induced spin-state trapping processes (LIESST),[2] single-crystal-to-single-crystal reactions[3] and the determination of transient molecular species.[4]

Systems undergoing solid-state linkage isomerism have attracted particular interest as the small but significant structural changes they involve are particularly well-suited to study via single-crystal photocrystallographic methods, where the preservation of crystal integrity throughout the experiment is paramount. A number of complexes have been shown to undergo photoconversion at low temperature to produce long-lived metastable isomers, and often conversion is found to be fully reversible on heating.[5] These observations have led authors to propose the application of such systems in several technological applications, including optical switches and holographic data storage devices,[6] and as such their development remains of key future interest.

The study of photoinduced metastable species using photocrystallographic techniques has been pioneered by Coppens, beginning with the successful identification of the two photo-excited species of sodium nitroprusside, MS_1 and MS_2, as distinct nitrosyl linkage isomers.[7] Subsequent studies by several research groups have involved different isomerising ligands and a variety of molecular systems,[8] and have highlighted the effect of the surrounding crystalline environment on the isomerisation.[9] While some interesting examples of metastable linkage isomers have now been reported, the question of what fundamental factors influence the progress of the isomerisation reaction remains the subject of some debate with arguments in support of steric[10] or electronic[11] control over photoconversion. In addition, it is acknowledged that a key limitation in the study of such species is the relatively low level of photoconversion achievable in the majority of single-crystal systems studied.[12] As a high level of conversion that is both reversible and controllable is important if materials are to have real potential for technological application, better knowledge of the processes influencing isomerisation is desirable.

In our efforts to gain a more complete understanding of the photochemical reaction in such systems we have investigated a number of transition metal complexes exhibiting solid-state nitro-nitrito linkage isomerism. As a result of studies aimed at improving photoconversion levels we reported the first fully-reversible nitro – nitrito isomerism in the complex $[Ni(dppe)(\eta^1\text{-}NO_2)Cl]$ (dppe = *bis*-1,2-diphenylphosphinoethane) upon photoactivation with UV LED light at temperatures below 160K.[13] Photocrystallographic evidence for the 100% conversion to the metastable isomer $[Ni(dppe)(\eta^1\text{-}ONO)Cl]$ was supported with data from solid-state Raman spectroscopy experiments. Subsequently we have found similar 100% reversible nitro – nitrito conversion in two analogous complexes involving bulky phosphine auxiliary ligands; $[Ni(dppe)(\eta^1\text{-}NO_2)_2]$ and $[Ni(dcpe)(\eta^1\text{-}NO_2)_2]$ (dcpe = *bis*-1,2-

Table 1 Crystal data and data collection and refinement parameters for ground state and photoactivated structures

Compound reference	**1**	**1#O**	**2**	**2#O**	**3**	**3#O**	**4**
Chemical formula	$C_{12}H_{30}N_2NiO_4P_2$	$C_{12}H_{30}N_2NiO_4P_2$	$C_{38}H_{34}Cl_4N_2O_4P_2Pd$	$C_{38}H_{34}Cl_4N_2O_4P_2Pd$	$C_{36}H_{30}As_2N_2O_4Pd$	$C_{36}H_{30}As_2N_2O_4Pd$	$C_{38}H_{34}Cl_4N_2O_4P_2Pt$
Formula Mass	387.03	387.03	892.81	892.81	810.86	810.86	981.50
Crystal system	Monoclinic	Monoclinic	Orthorhombic	Orthorhombic	Triclinic	Triclinic	Orthorhombic
a/Å	7.839(4)	7.890(4)	20.690(18)	20.629(10)	9.5940(7)	9.5967(9)	20.471(5)
b/Å	7.814(4)	7.787(3)	8.069(7)	7.985(4)	9.9987(7)	9.9479(9)	7.953(5)
c/Å	15.152(11)	15.251(6)	23.51(2)	23.339(12)	10.1274(7)	10.1121(9)	23.261(5)
α/°	90.00	90.00	90.00	90.00	111.490(1)	111.262(1)	90.00
β/°	95.15(4)	94.82(2)	90.00	90.00	90.473(1)	90.931(1)	90.00
γ/°	90.00	90.00	90.00	90.00	115.209(1)	114.454(1)	90.00
Unit cell volume/Å^3	924.4(9)	933.6(7)	3925(6)	3845(3)	802.14(10)	803.05(13)	3787(3)
Temperature/K	100(2)	100(2)	100(2)	100(2)	100(2)	100(2)	100(2)
Space group	$P2_1/c$	$P2_1/c$	*Pbca*	*Pbca*	$P\bar{1}$	$P\bar{1}$	*Pbca*
No. of formula units per unit cell, *Z*	2	2	4	4	1	1	4
% activation	0	25(1)	0	46(1)	0	39(1)	0
No. of reflections measured	9601	9782	33795	38812	10978	11526	6847
No. of independent reflections	2731	2743	5807	5879	4729	4795	2820
R_{int}	0.0523	0.0271	0.0941	0.0742	0.0536	0.0470	0.0340
Final R_1 values ($I > 2\sigma(I)$)	0.0443	0.0287	0.0560	0.0391	0.0524	0.0366	0.0185
Final $wR(F^2)$ values ($I > 2\sigma(I)$)	0.0929	0.0718	0.1514	0.1015	0.1589	0.1032	0.0298
Final R_1 values (all data)	0.0494	0.0327	0.0645	0.0482	0.0545	0.0397	0.0728
Final $wR(F^2)$ values (all data)	0.0946	0.0735	0.1627	0.1089	0.1621	0.1061	0.0338
Goodness of fit on F^2	1.206	1.035	1.007	1.062	1.003	1.065	0.765

dicyclohexylphosphinoethane).[14] Complementing these square-planar phosphino systems, we have also investigated photoisomerisation in a series of octahedral nickel-nitro complexes containing bidentate amine co-ligands.[15] In addition we have reported the interesting behaviour of the tridentate amine complex [Ni(Et$_4$dien)(η^1-NO$_2$)$_2$], which undergoes reversible nitro-nitrito linkage isomerism following exposure to both UV light and heat,[16] and have also observed similar behaviour in the system [Pd(papaverine)(PPh$_3$)(NO$_2$)] on exposure to both of these stimuli.[17] These results indicate that the nature of the surrounding crystalline environment has an effect on the photochemical reaction, in-line with previous findings.[9]

While our previous work has centred on systems involving *cis*-oriented, bidentate auxiliary ligands, we now present the results of an investigation into the effect of co-ligands bound *trans* to the isomerising nitrite groups. We herein report the solid-state photochemical reactivity of a set of analogous Group 10 metal-nitro complexes with *trans*-monodentate auxiliary ligands, which show high levels of photoconversion under photocrystallographic conditions.

Experimental

Complexes [Ni(PEt$_3$)$_2$(NO$_2$)$_2$] **1**, [Pd(PPh$_3$)$_2$(NO$_2$)$_2$] **2** and [Pd(AsPh$_3$)$_2$(NO$_2$)$_2$] **3** have been reported previously and were prepared by the established literature methods,[18] and characterized initially by spectroscopic methods and satisfactory microanalyses. The complex [Pt(PPh$_3$)$_2$(NO$_2$)$_2$] **4** was prepared by a modification of a literature method[19] which involved the treatment of a freshly prepared sample of potassium tetranitroplatinate (0.1 g, 0.219 mmol) with two equivalents of triphenylphosphine (0.123 g, 0.438 mmol) in acetone (10 mL) and the mixture stirred for 24 h. The initial homogeneous solution turned cloudy, rapidly, and the precipitate collected by filtration. The solid was dissolved in dichloromethane was filtered to remove the potassium nitrite. Crystals suitable for the X-ray crystallographic experiments were grown from dichloromethane solution layered with acetonitrile. Yield: 83% (0.148 g, 0.18 mmol).

X-ray diffraction investigations for complexes **2** and **3** were carried out on Station 11.3.1 of The Advanced Light Source (ALS), Lawrence Berkeley National Laboratory[20] and for complex **1** on Station 9.8 of Daresbury Synchrotron Radiation Source.[21] Single-crystal X-ray data collections were carried out on Bruker APEXII CCD diffractometers[22] equipped with an Oxford Cryosystems cryostream cooling device.[23] Data for complex **4** was recorded on an Agilent Gemini A-Ultra diffractometer[24] at the University of Bath using Mo-K_α radiation, the crystal being cooled by an Agilent Cryojet.[25] The structures were solved and refined using SHELXL.[26] Least squares refinement was carried out based on F^2. All non-hydrogen atoms were refined on anisotropic displacement parameters except for the partially occupied components of the nitro groups in the photoactivated structures. Hydrogen atoms on the ethyl and phenyl groups were placed in idealized positions and allowed to ride on the relevant carbon atoms, with isotropic displacement parameters set at *1.2 U* of the carbon atom to which they were attached. Refinement continued until convergence was reached. Crystal data and refinement parameters for the ground and photoactivated structures are presented in Table 1.

Suitable single crystals were mounted on the diffractometer and cooled to 100 K. Ground state structures ("dark") were

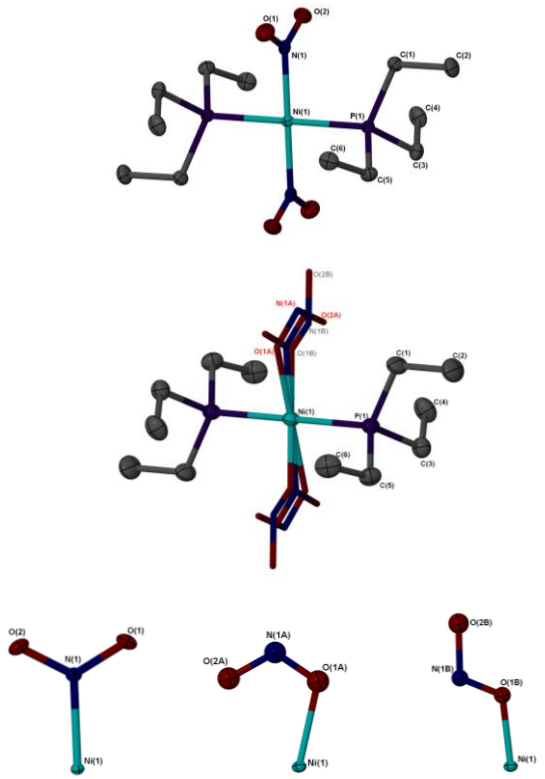

Fig. 1 (a) Ground state structure of **1**. (b) Photoactivated structure 1#O showing the 16% *endo* and 9% *exo* excited state forms and the remaining ground state component. (c) Close up of the nitrite group in 1#O for each individual component. Ellipsoids are plotted at 50 % probablity where shown

collected with no external light. The crystals were then irradiated *in situ* using a ring of 6 LEDs.[27] Irradiation of the single crystals in different experiments was carried out using blue or UV LEDs (UV: 400 nm, 350 mcd; blue: 470 nm, 3300 mcd). During the exposure the crystal was continuously rotated to maximize the uniformity of radiation. After exposure a second dataset ("light") was collected and the level of photo-activation conversion was assessed through structure solution and refined with the nitro and nitrito components being treated as a disorder model with the total occupancy of each atom being summed to unity. The process of irradiation, dataset collection, solving and refining of the crystal structure was repeated until the maximum level of conversion to the nitrito complex was achieved. The crystal structure was then measured at different temperatures in 10 K intervals between 100-220 K to assess the temperature range over which the metastable state was present.

All DFT calculations were performed using the B3LYP[28] hybrid density functional under the Gaussian 03 package.[29] Transition states were obtained using the UB3LYP functional ('guess=mix') and the STQN method. Geometry optimisations were performed using a quasi-relativistic pseudopotential and associated basis set (SDD) for platinum,[30] and a 6-31G(d)[31] basis set for all other atoms. Frequency calculations were performed at the optimised geometries to confirm the nature of the stationary points, and quoted freqencies were scaled by a factor of 0.96.[32] Electronic transitions (TD-DFT) and single point energies ('tight' convergence criteria) were calculated at the optimised geometries using the SDD basis set augmented with two f-polarisation functions[33] for platinum and the 6-311G(2d,p)[34] basis set for all other atoms. Molecular orbitals were calculated at the 6-311G(2d,p) level and visualised using the Molekel program package.[35] Transition state energies were corrected for triplet contamination using spin projection methods.[36]

Results and discussion

The complex $[Ni(PEt_3)_2(NO_2)_2]$ **1**, which had not been crystallographically characterised previously, crystallises in the monoclinic space group $P2_1/c$ following slow evaporation from a dichloromethane / toluene mixture. The crystal structure determination confirms the *trans* arrangement of the pairs of nitro and phosphine ligands and that the NO_2 groups are η^1-N bound. The nickel atom, adopting near-perfect square planar geometry, sits on an inversion centre and is bound to one crystallographically independent triethylphosphine group and one nitrite ligand (Figure 1a).

For photocrystallographic experiments a suitable single crystal was mounted on the diffractometer and first cooled to 100 K in the absence of any light, before a high resolution X-ray dataset was collected. The structure was subsequently solved and refined to show that the nitro ligand adopts a fully nitro-(η^1-NO_2) configuration in this initial, ground state structure. The same crystal was then held at 100 K on the diffractometer and irradiated with UV LED light using a specially designed LED ring.[27] The ring positions six LEDs *c.a.* 1 cm from the crystal in a uniform circle, helping to ensure that the whole sample is irradiated evenly throughout. After a period of 10 minutes the UV light was switched off and a second, identical data collection was conducted at 100 K. This second dataset revealed that linkage isomerism had occurred in the nitrite group, with a total 25% of the crystal converted to nitrito-(η^1-ONO) configuration (**1#O**) while the remaining 75% retains the initial nitro-(η^1-NO_2) arrangement. The nitrito-(η^1-ONO) excited state is made up of two individual components; an *endo*-(η^1-ONO) component at 16% occupancy, and an *exo*-(η^1-ONO) component at 9% occupancy (Figure 1b). The photoactivated species remains present when the crystal is held at 100 K in the dark, confirming the excited state to be metastable under these conditions. Unfortunately, further irradiation with UV light caused the crystal to decompose, therefore 25 % is the maximum level of excitation that can be confirmed for this species. The same level of conversion was achieved with a second sample, confirming the result to be repeatable, and finally variable temperature parametric studies were conducted in order to ascertain the temperature range over which the photoactivated species is metastable. Datasets were collected at regular temperature intervals as the crystal was heated *in-situ* on the diffractometer and the metastable state was found to exist up to 220 K, above which the system reverts back to its initial nitro-(η^1-NO_2) arrangement.

Analysis of the crystal packing using the Cambridge

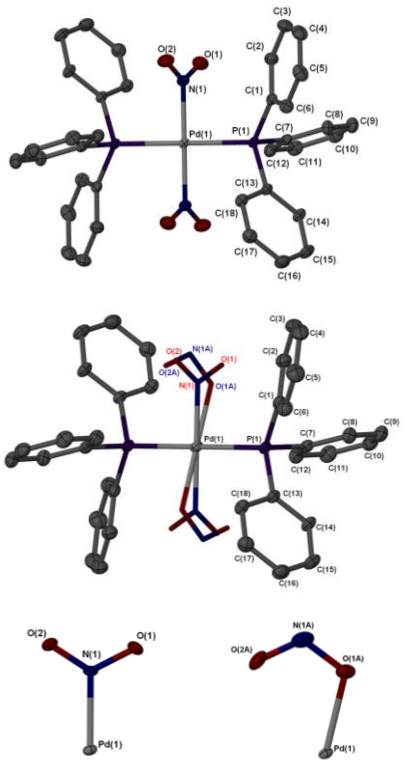

Fig. 2 (a) Ground state structure of 2. (b) Photoactivated structure 2#O showing the 46% endo component and the remaining ground state. (c) Close up of the nitrite group in 2#O for each component. Ellipsoids are plotted at 50 % probablity where shown**.**

Crystallographic Data Centre software Mercury[37] shows that **1** adopts a tightly-packed arrangement. Employing the default settings for the software, that a volume with a radius larger than 1.20 Å constitutes a void in the crystal structure, no void space is calculated to exist in either **1** or **1#O**. Calculations were also run using Mercury's Crystal Packing Similarity tool, which calculates the degree to which the crystal packing in two structures are the same by analysing the geometries of a cluster of molecules.[37] All of the molecular geometries in **1** and **1#O** are found to match and the software calculates an RMS deviation of 0.065 between the two structures (comparing a *default* cluster of 15 molecules), strongly indicating that the crystal packing remains unchanged between the ground and photoexcited states. Further supporting this observation, analysis of the intermolecular interactions in both structures using the program CrystalExplorer[38] indicates changes are confined to interactions involving the isomerising nitrite group (see Supporting Information). In addition, only a very small volume increase of 1.0% was determined following the isomerisation. All of the above analysis indicates that there is very little free space in the static crystal structure within which the nitro – nitrito conversion can occur, suggesting that an argument for purely steric control of the photoreaction is unlikely. However, considering that atomic rearrangement is required in order for isomerisation to occur, it seems likely that steric factors must make some contribution. It might be argued that the observed crystal decomposition following prolonged light exposure, preventing higher levels of conversion in **1**, is the result of steric effects in the crystal lattice. The triethylphosphine co-ligands are fairly small with the isomerising nitrite group making up *c.a.* 15% of the total molecular volume. It is possible therefore that further conversion above 25% induced too much strain in the overall lattice, compromising single crystal integrity.

A photocrystallographic study of $[Pd(PPh_3)_2(NO_2)_2]$ **2** was next conducted, following the same procedure as that outlined for **1**. The crystal structure of 2 has been reported previously establishing the *trans* arrangements of the pairs of nitro and phosphine groups.[18b]

In the ground state structure at 100 K (Figure 2(a)), **2** crystallises in the orthorhombic space group *P*bca as a dichloromethane solvate. Again, the metal centre sits on an inversion centre, so that the asymmetric unit consists of half a molecule of **2** and one dichloromethane solvent molecule. The palladium atom adopts perfect square-planar geometry and the nitro group is bound in 100 % nitro-(η^1-NO_2) configuration.

In order to take into account energy differences in the UV/visible absorption spectra of **1** and **2**, photoactivation of **2** was attempted using both 400 nm and lower wavelength 362 nm LED light. While an excitation of only 30% was achieved at 400 nm, a maximum 46% nitro – nitrito conversion was achieved after 288 minutes irradiation using 362 nm light. The resulting excited state structure, **2#O** (Figure 2(b)) shows that the photoactivated species nitrito-(η^1-ONO) adopts a single *endo* orientation, with no evidence of the *exo* form in the Fourier electron density difference maps. Further irradiation produced no appreciable change, showing that a photostationary state had been reached. The photoactivated species was confirmed to be metastable as it remained when the crystal was held in the dark at 100 K. Variable temperature parametric studies were then conducted, determining that the nitrito-(η^1-ONO) isomer exists on heating to a temperature of 240 K, above which the system returns to its ground state nitro-(η^1-NO_2) configuration.

Analysis with Mercury again shows that **2** adopts a fairly tight packing arrangement with the only free channels in the crystal structure, running parallel to the *b*-axis, filled by the dichloromethane solvent molecules, meaning that no void space is calculated to exist in the lattice. Calculations with the Crystal Packing Similarity tool find that the molecular geometries molecules match. A RMS deviation of 0.111 is obtained when **2** and **2#O** are compared, with the small deviations between the structures confined to the phenyl moieties and dichloromethane solvent molecules. Additional analysis of the intermolecular interactions in both **2** and **2#O** using CrystalExplorer also confirm there to be little difference in the overall crystal structure following photoactivation, excepting changes in the interactions involving atoms of the isomerising group (see Supporting Information). Combined with a small 2.0% decrease in cell volume observed on going from the ground state to the photoexcited structure, the analysis again infers that a purely steric argument to explain the linkage isomerisation reaction in **2** would be inadequate.

The molecular and crystal structure of $[Pd(AsPh_3)_2(NO_2)_2]$

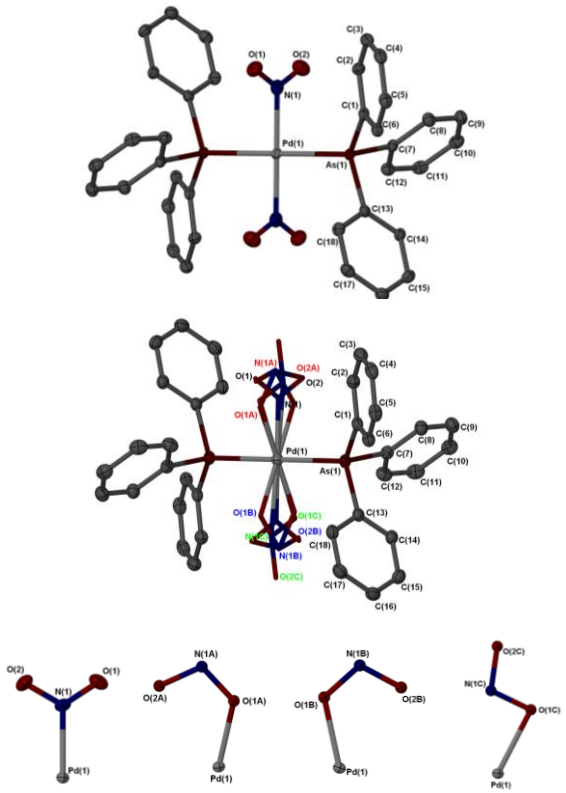

Fig. 3 (a) Ground state structure of 3. (b) Photoactivated structure 3#O showing the 19 % and 13 % *endo* form, 8 % *exo* form and the remaining ground state component. (c) Close up of the nitrite group in 3#O for each component. Ellipsoids are plotted at 50 % probablity where shown

3 has not been reported previously. The complex crystallises in the triclinic space group *P*-1 following slow evaporation from dichloromethane. The metal atom is again positioned on the inversion centre and adopts square planar geometry, with the crystallographically unique nitrite and triphenylarsine ligands positioned *cis* to one another (Figure 3(a)) such that the pairs of nitro and arsine ligands are *trans* to each other. The nitrite ligand adopts solely nitro-(η^1-NO_2) coordination in the ground state structure, determined at 100 K in the absence of any light.

A photocrystallographic study of **3** was conducted at 200 K, as described for both **1** and **2**. After 300 min exposure to UV LED light a total 40% of the crystal had undergone nitro – nitrito conversion, displaying similar behaviour to that of the analogous complex **2**. The photoactivated nitrito-(η^1-ONO) species comprises of three separate components: two disordered *endo*-(η^1-ONO) configurations with occupancies of 19% and 12%; and one *exo*-(η^1-ONO) component at 8% occupancy (Figure 3(b), **3#O**). Prolonged exposure to UV light at 100 K produced no further change, confirming that the system had reached its photostationary state. The photoactivated species remained present after the crystal was held in the dark at 100 K, confirming the system to be metastable under these conditions. Variable temperature parametric studies indicate that, as for the analogous complex **2**, the metastable state is still detected at temperatures between 100 and 240 K. However, at temperatures above 240 K the system returns to its 100% nitro-(η^1-NO_2) ground state configuration.

Analysis of steric factors inferred from the crystal structure of **3** again provides similar conclusions as those for **1** and **2**. Molecules of **3** are packed tightly in the single crystal, with calculations confirming that no free void space exists in the lattice for either **3** or **3#O**. In a comparison of the crystal packing similarities between the two structures, the calculation using Mercury shows that geometries of all the investigated molecules are similar and there is an RMS deviation of 0.083 between the two crystal packing arrangements. Analysis with CrystalExplorer also confirms once more that there is little difference between the intermolecular interactions observed in the structures of **3** and **3#O**, with the only discernible changes being in O…H close contacts that can be rationalised as the result of nitro – nitrito conversion following photoactivation (Supporting Information). With the additional observation that the unit cell volume changes by just 0.2% upon excitation, the behaviour of **3** again indicates that the linkage isomerism reaction must be affected by other factors in addition to steric influences within the single crystal.

The complex $[Pt(PPh_3)_2(NO_2)_2]$ **4** crystallises in the orthorhombic space group *Pbca* with half a molecule and one dichloromethane solvent molecule in the asymmetric unit (Figure 4). As for the other complexes the platinum centre sits on an inversion centre, has a square planar geometry, and is bound to symmetry related, *trans* orientated pairs of nitro and phosphine ligands. From a ground state data collection conducted at 100 K in the dark, the nitrite ligand is observed to adopt a 100 % nitro-(η^1-NO_2) configuration. A photocrystallographic investigation was conducted for **4** following the procedure outlined previously. A suitable single crystal was irradiated with UV LED light at 100 K over a prolonged period, with data collections conducted at 1 h intervals. The subsequent X-ray structures show little deviation from the ground state with the nitrite group clearly adopting nitro-(η^1-NO_2) configuration, giving no evidence of a photo-induced species in **4** using UV LED light.

Gas phase DFT calculations were performed to determine the predicted electronic properties of compounds **1** to **4**. Although gas phase calculations and solid state data cannot be compared directly, a comparison of theoretical results with experimental data may help to explain the observed photochemical behaviour of the complexes, and qualitatively assess the contribution of electronic effects on nitro – nitrito photoactivation.

Calculations predict the HOMO to have a major contribution from the nitro group in all four complexes (89% contribution or above), and it is therefore consistent that an excitation from this orbital could have an effect on the ligand and its coordination geometry. The major electronic transitions predicted from TD-DFT calculations, in all cases performed on geometry optimised ground state structures, compare well to the major absorption peaks observed experimentally for solution UV/vis spectra of all four complexes (Supporting Information).

Results for the analogous complexes **2** and **3** show that the

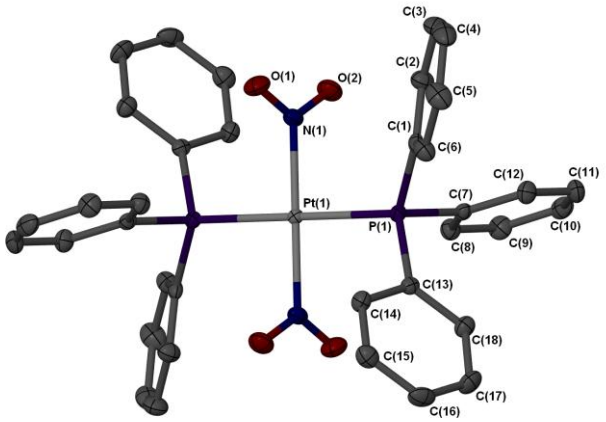

Fig. 4 The molecular structure of **4** drawn with 50% displacement ellipsoids.

main electronic transitions predicted from TD-DFT calculations occur at approximately the same wavelength, while additionally the frontier molecular orbitals are identical in shape and are calculated to consist of very similar contributions from the metal atoms, nitro and auxiliary ligand (Supporting Information). The close agreement in theoretical results is consistent with the very similar photochemical behaviour determined experimentally for these two complexes, and suggests that the change in the auxiliary ligands to a heavier donor atom has little effect either the electronic or photochemical properties of the system.

Comparison of both the experimental UV/vis spectra and the major electronic transition peak determined from TD-DFT calculations for the analogous complexes **2** and **4** show a shift to lower wavelength on moving to the heavier transition metal centre. In addition, the UV/visible spectrum of **1** has an absorption tail that extends further into the visible region than those of **2**, **3**, and **4**, suggesting that it would be more receptive to longer wavelength light that either of its palladium or platinum analogues (Supporting Information). This is consistent with the idea that the kinetic lability of the nitro ligand decreases with the heavier transition metal, and offers an electronic explanation for the *lower* observed photoconversion in **4** with UV LED light.

Conclusions

The results into the single crystal photocrystallographic studies of the four *trans* complexes $[Ni(PEt_3)_2(NO_2)_2]$ **1**, $[Pd(PPh_3)_2(NO_2)_2]$ **2**, $[Pd(AsPh_3)_2(NO_2)_2]$ **3** and $[Pt(PPh_3)_2(NO_2)_2]$ **4** show significant variations in the level of conversion from the η^1-NO_2 nitro form to the η^1-ONO nitrito form depending on the metal present. Complex **1** underwent 25% conversion to the nitrito form before crystal decomposition occurred. This contrasts the 100% conversion recently obtained for the closely related *cis* di-nitro complex, $[Ni(dppe)(\eta^1\text{-}NO_2)Cl]$.[13] For **1** it seems that steric factors dominate as the crystal decomposition, presumably the result of strain being induced within the crystal, prevents a higher conversion.

Complexes **2** and **3** underwent 46% and 39% conversion, respectively, to the nitrito form when a photostationary state was reached. This is also in contrast with the conversion obtained for **1**, but it is unfortunate that a direct comparison cannot be made, as it was not possible to obtain suitable single crystals of the exactly analogous $[Ni(PPh_3)_2(NO_2)_2]$ complex. However, the conversion levels for the two palladium complexes are considerably lower than for the *cis* di-nitro complex, $[Ni(dppe)(\eta^1\text{-}NO_2)Cl]$. The similarity in the excitation levels obtained for the phosphine and arsine derivatives suggest that the auxiliary ligands have little influence on the level of conversion.

Using the same experimental conditions, UV visible light, and a crystal temperature of 100 K, **4** did not show any apparent isomerization from the η^1-NO_2 nitro form to the η^1-ONO nitrito form. Although the solution UV/visible spectra of the four complexes show a shift in the absorption bands, it should still be possible to photoactivate the η^1-NO_2 nitro groups in each case. Therefore, the difference in the level of photoactivation observed for the Pd and Pt complexes may relate to the greater kinetic inertness of the Pt complex, **4**, compared to the related Pd complexes, **2** and **3**. These results may suggest that kinetic as well as steric factors may be important when designing complexes that are required to undergo high levels of photoactivated linkage isomerism in the solid state. Further supporting the view that steric factors may not be solely responsible for the behaviour of these complexes in the solid state under photoactivation is the consideration of the size of the "reaction cavity" in these systems. The "reaction cavity", as defined by Ohashi,[39] is the volume of space within the crystal occupied by the NO_2 group. This volume can be calculated by removing the NO_2 coordinates from the crystal structures and calculating the void space using the Crystallographic Data Centre software Mercury.[37] Using a 1.2 Å void radius and a 0.1 grid, the percentage of the molecular volume occupied by the NO_2 was 14.2% (**1**), 6.1% (**2**), 8.1% (**3**) and 4.6% (**4**). Clearly, the volume available does not correlate directly with the percentage conversion achieved on photoactivation. Thus, factors other than the size of the reaction cavity must be playing a part in the isomerization process.

Acknowledgements

We thank the EPSRC for financial support for the project (EP/D058147 and EP/D054397) and for studentships to L. E. H., S. S., C. H. W. and M. R. W. and for a Senior Research Fellowship to P. R. R. Professor Philip Coppens, SUNY Buffalo, are thanked for helpful discussions. We are grateful to the STFC Daresbury Laboratory and the ALS, Lawrence Berkeley National Laboratory for the award of beamtime.

Notes and references

[a] *Department of Chemistry, University of Bath, Claverton Down, Bath, UK BA2 7AY. Fax: +441225 386231; Tel: 01225 383183; E-mail: p.r.raithby@bath.ac.uk*
[b] *Advanced Light Source, Lawrence Berkeley National Laboratory, 1 cyclotron road, Berkeley CA94720, USA.*
[c] *STFC Daresbury Laboratory, Daresbury, Warrington, UK WA4 4AD.*

† Electronic Supplementary Information (ESI) available: [details of any supplementary information available should be included here]. See DOI: 10.1039/b000000x/

1. P. Coppens, B. Iversen and F. K. Larsen, *Coord. Chem. Rev*., 2005, **249**, 179..
2. a) A. L. Thompson, V. A. Money, A. E. Goeta and J. A. K. Howard, *Comptes Rendus Chimie*, 2005, **8**, 1365; b) P. Gutlich, Y. Garcia and T. Woike, *Coord. Chem. Rev*., 2001, **219**, 839; c) M. A. Halcrow, *Polyhedron*, 2007, **26**, 3523; d) S. Pillet, V. Legrand, H.-P. Weber, M. Souhassou, J.-F. Létard, P. Guionneau and C. Lecomte, *Zeit. Krist.*, 2008, **223**, 235; e) F. Varret, K. Boukheddaden, A. Goujon, B. Gillon and G. J. McIntyre, *Zeit. Krist.*, 2008, **223**, 250.
3. a) S. K. Brayshaw, S. Schiffers, A. J. Stevenson, S. J. Teat, M. R. Warren, R. D. Bennett, I. V. Sazanovich, A. R. Buckley, J. A. Weinstein and P. R. Raithby, *Chem.-Eur. J*., 2011, **17**, 4385; b) M. F. Mahon, P. R. Raithby and H. A. Sparkes, *Crystengcomm*, 2008, **10**, 573; c) S. L. Zheng, M. Messerschmidt and P. Coppens, *Chem. Commun*., 2007, 2735; d) Y. Nishioka, T. Yamaguchi, M. Kawano and M. Fujita, *J. Am. Chem. Soc*., 2008, **130**, 8160.
4. a) M. Kawano and M. Fujita, *Coord. Chem. Rev*., 2007, **251**, 2592; b) P. Coppens, O. Gerlits, I. I. Vorontsov, A. Y. Kovalevsky, Y.-S. Chen, T. Graber, M. Gembicky and I. V. Novozhilova, *Chem. Comm*., 2004, 2144; c) C. D. Kim, S. Pillet, G. Wu, W. K. Fullagar and P. Coppens, *Acta Crystallogr. Sect. A*, 2002, **58**, 133.
5. P. Coppens, I. Novozhilova and A. Kovalevsky, *Chem. Rev*., 2002, **102**, 861.
6. a) D. Schaniel, M. Imlau, T. Weisemoeller, T. Woike, K. W. Kramer and H. U. Gudel, *Adv. Mater*., 2007, **19,** 723; b) M. Goulkov, D. Schaniel and T. Woike, *J. Opt. Soc. Am. B*, 2010, **27**, 927; c) A. Zangl, P. Klufers, D. Schaniel and T. Woike, *Inorg. Chem. Comm*., 2009, **12**, 1064.
7. M. D. Carducci, M. R. Pressprich and P. Coppens, *J. Am. Chem. Soc*., 1997, **119**, 2669.
8. a) A. E. Phillips, J. M. Cole, T. d'Almeida and K. S. Low, *Inorg. Chem*., 2012, **51**, 1204; b) J. M. Cole, *Analyst*, 2011, **136**, 448; c) A. E. Phillips, J. M. Cole, T. d'Almeida and K. S. Low, *Phys. Rev. B*, 2010, **82**, 155118; d) K. F. Bowes, J. M. Cole, S. L. G. Husheer, P. R. Raithby, T. L. Savarese, H. A. Sparkes, S. J. Teat and J. E. Warren, *Chem. Commun*., 2006, 2448; e) A. Y. Kovalevsky, G. King, K. A. Bagley and P. Coppens, *Chem.-Eur. J*., 2005, **11**, 7254; f) A. Y. Kovalevsky, K. A. Bagley, J. M. Cole and P. Coppens, *Inorg. Chem*., 2003, **42**, 140.
9. S. L. Zheng, M. Gembicky, M. Messerschmidt, P. M. Dominiak and P. Coppens, *Inorg. Chem*., 2006, **45**, 9281.
10. B. Q. Ma, Y. G. Zhang and P. Coppens, *Cryst. Growth Des*., 2002, **2**, 7.
11. D. Schaniel and T. Woike, *Phys. Chem. Chem. Phys*., 2009, **11**, 4391..
12. P. R. Raithby, *Crystallography Reviews*, 2007, **13**, 121.
13. M. R. Warren, S. K. Brayshaw, A. L. Johnson, S. Schiffers, P. R. Raithby, T. L. Easun, M. W. George, J. E. Warren and S. J. Teat, *Angew. Chem.-Int. Edit.*, 2009, **48**, 5711.
14. M. R. Warren, Easun, T. L., Brayshaw, S. K., Deeth, R. J., George, M. W., Johnson, A. L., Raithby, P. R., Schiffers, S., Stevenson, A. J., Teat, S. J., Warren, J. E., Woodall, C. H, *Chem. Sci*., 2012, in preparation.
15. S. K. Brayshaw, T. L. Easun, M. W. George, A. M. E. Griffin, A. L. Johnson, P. R. Raithby, T. L. Savarese, S. Schiffers, J. E. Warren, M. R. Warren and S. J. Teat, *Dalton Trans*., 2012, **41**, 90.
16. L. E. Hatcher, M. R. Warren, D. R. Allan, S. K. Brayshaw, A. L. Johnson, S. Fuertes, S. Schiffers, A. J. Stevenson, S. J. Teat, C. H. Woodall and P. R. Raithby, *Angew. Chem. Int. Edn*., 2011, **50**, 8371..
17. S. E. Bajwa, T. E. Storr, L. E. Hatcher, T. J. Williams,, C. G. Baumann, A. C. Whitwood, D. R. Allan, S. J. Teat, and. P. R. Raithby and I. J. S. Fairlamb, *Chem. Sci*., 2012, c2sc01050j.
18. a) D. T. Doughty, G. Gordon and R. P. Stewart, *J. Am. Chem. Soc*., 1979, **101**, 2645; b) L. M. Tack, J. L. Hubbard, G. R. Kriek, J. Dubrawski, J. H. Enemark, *Cryst. Struct. Comm*., 1981, **10**, 385; c) D. M. L. Goodgame and M. A. Hitchman, *Inorg. Chem*., 1966, **5**, 1303.
19. L. A. Rigamonti, M. Forni; M. Manassero; C. Manassero and A. Pasini, *Inorg. Chem*., 2010, **49**, 123.
20. Station13.3.1, The Advanced Light Source www.als.lbl.gov/als/techspecs/bl11.3.1.html.
21. Station 9.8, Daresbury Synchrotron Radiation Source www.srs.ac.uk/srs/stations/station9.8.htm.
22. SMART and SAINT Software Reference Manuals,. Version 6.22., Bruker AXS Analytic X-ray Systems Inc, Madison, WI 2000, 2001.
23. Oxford Cryosystems Cryostream 700 series, http://www.oxfordcryosystems.co.uk/cryostream/700series.htm.
24. Agilent Gemini A-Ultra Diffractometer http://www.chem.agilent.com/en-US/Products/Instruments/x-raycrystallography/smallmoleculesystem/geminiultra/pages/default.aspx.
25. Agilent CryojetXL http://www.chem.agilent.com/en-US/Products/Instruments/x-raycrystallography/accessories/cryojetxl/pages/default.aspx.
26. G. M. Sheldrick, *Acta Crystallogr. Sect. A*, 2008, **64**, 112.
27. S. K. Brayshaw, J. W. Knight, P. R. Raithby, T. L. Savarese, S. Schiffers, S. J. Teat, J. E. Warren and M. R. Warren, *J. Appl. Crystallogr*., 2010, **43**, 337.
28. a) C. Lee, W. Yang and R. G. Parr, *Phys. Rev. B*, 1988, **37**, 785; b) A. D. Becke, *J. Chem. Phys*., 1993, **98**, 5648.
29. M. J. Frisch, M. J. Frisch et al. Gaussian, Inc., Wallingford CT, Editon edn., 2004, pp. Gaussian 03, Rev D.01, M. J. Frisch et al. Gaussian, Inc., Wallingford CT.
30. D. Andrae, U. Haussermann, M. Dolg, H. Stoll and H. Preuss, *Theor. Chem. Acc*., 1990, **77**, 123.
31. a) R. Ditchfield, W. J. Hehre and J. A. Pople, *J. Chem. Phys*., 1971, **54**, 724; b) P. C. Hariharan and J. A. Pople, *Theor. Chem. Acta*., 1973, **28**, 213.
32. A. P. Scott and L. Radom, *J. Phys. Chem*., 1996, **100**, 16502.
33. J. M. L. Martin and A. Sundermann, *J. Chem. Phys*., 2001, **114**, 3408.
34. R. Krishnan, J. S. Binkley, R. Seeger and J. A. Pople, *J. Chem. Phys*., 1980, **72**, 650.
35. U. Varetto, Editon edn., 2009, pp. MOLEKEL 5.4, Varetto, U. Swiss National Supercomputing Centre: Manno (Switzerland).
36. a) S. Yamanaka, T. Kawakami, H. Nagao and K. Yamaguchi, *Chem. Phys. Lett*., 1994, **231**, 25; b) K. Yamaguchi, F. Jensen, A. Dorigo and K. N. Houk, *Chem. Phys. Lett.*, 1988, **149**, 537.
37. C. F. Macrae, I. J. Bruno, J. A. Chisholm, P. R. Edgington P. McCabe, E. Pidcock, L. Rodriguez-Monge, R. Taylor, J. van de Streek and P. A. Wood, *J. Appl. Cryst*., 2008, **41**, 466..
38. J. J. McKinnon, M. A. Spackman and A. S. Mitchell, *Acta Crystallogr. Sect. B*, 2004, **60**, 627.
39. Y. Ohashi, K. Yanagi, T. Kurihara, Y. Sasada and Y. Ohgo, *J. Am. Chem. Soc*., 1981, **103**, 5805.